Fault system of the 2004 Mid-Niigata Prefecture Earthquake and its aftershocks

Naoshi Hirata[1], Hiroshi Sato[2], Shin'ichi Sakai[3], Aitaro Kato[4], Eiji Kurashimo[5]

The Earthquake Research Institute, the University of Tokyo

1-1-1 Yayoi Bunkyo-ku Tokyo 113-0032, Japan
Phone: +81-3-3818-3697
FAX: +81-3-5689-7234

1) e-mail:hirata@eri.u-tokyo.ac.jp
2) e-mail:satow@eri.u-tokyo.ac.jp
3) e-mail:coco@eri.u-tokyo.ac.jp
4) e-mail:akato@eri.u-tokyo.ac.jp
5) e-mail:ekura@eri.u-tokyo.ac.jp

Submitted to Landslides on January 6, 2005

Revised on March 27; Accepted on March 28, 2005

will be published in Landslides Vol.2(2)

Abstract

Data recorded by a seismic network deployed the day after the 2004 Mid-Niigata Prefecture Earthquake (M 6.8) in central Japan are used to determine the major source faults responsible for the mainshock and major aftershocks. Using this high-resolution seismic data, three major source faults are identified: two parallel faults dipping steeply to the west located 5 km apart, and the other dipping eastward and oriented perpendicular to the west-dipping faults. The analysis also reveals that the lateral variation in seismic velocity observed at the surface extends to a depth of 15 km, encompassing the source area of the mainshock. This strong heterogeneity of the crust, related to the complex geological and tectonic evolution of the area, is considered to be responsible for the prominent aftershock activity following the 2004 Niigata event.

Keywords: Fault system, shallow earthquake, aftershock activity, Niigata, Japan

Introduction

The 2004 Mid-Niigata Prefecture Earthquake (Japan Metrological Agency; JMA), central Japan, was a damaging event that destroyed up to 10 000 dwellings, with 40 fatalities and leaving 3000 injured. The earthquake occurred at 17:56 (Japan Standard Time) on October 23, 2004 with a local body wave magnitude (M_{JMA}) of 6.8. The hypocenter was located at relatively shallow depth (13 km; JMA) in an active fault-and-fold system overlain by thick sediments (Fig. 1). JMA earthquake intensities of 7.0 were recorded in Kawaguchi and Ojiya. The event was followed by prominent aftershock activity, with five major aftershocks of M 5.5 or greater on the 23rd, and others on the 25th (M 5.8), 27th (M 6.1) and November 8 (M 5.9), more than twice as many as occurred in the disastrous 1995 Hyogo-ken Nanbu (Kobe) earthquake (Hirata et al., 1996). This succession of strong aftershocks caused further damage and hindered rescue and restoration activities. Although the event generated many fissures and landslides, only minor surface faulting (Maryuyama et al., 2005) was observed, and the western Nagaoka plain active fault, one of the 98 major active faults reported by the Japanese Government (Headquarters for Earthquake Research Promotion, 1999) did not exhibit any activity during this event, despite lying only 10 km to the west of the epicenter (Fig. 2).

Immediately following the mainshock, a temporary seismic array was deployed in the epicenter region to capture detailed aftershock data for analysis of the faulting mechanism. Although Japan has one of the densest arrays of seismic stations in the world (Obara, 2000), the average spacing between permanent telemetry stations is about 20 km, which is insufficient to precisely locate events shallower than 15 km. In particular, in areas where the lateral variation of velocity is severe, as in the area of the

Mid-Niigata Prefecture Earthquake, routine determination of the hypocenter using a one-dimensional velocity model with data from the permanent stations may include systematic bias in both epicenter location and depth. The data from the temporary high-resolution network deployed immediately after the mainshock are expected to reveal the source area of the mainshock and its migration in the aftershock succession.

Aftershock Observation

Deployment of battery-operated seismographs by the Earthquake Research Institute (ERI) began the day after the mainshock, and the installation of all 14 stations was completed within 46 h of the main event (Earthquake Research Institute, 2004; Sakai et al, 2005; Kato et al., 2005). The installation of self-powered seismographs was essential, as most were deployed in areas without power or usable infrastructure. Each station consisted of a three-component geophone and continuous digital data recorder, with the Global Position System (GPS) receiver for maintenance of the internal clock (accuracy of approx. 1 ms). Over several days following the mainshock, a further 150 seismic stations were deployed by many Japanese institutions, including ERI, to obtain detailed seismic data for the earthquake source area (e.g., Coordinate Committee for Earthquake Prediction Research, 2004). The report presents the data obtained by our rapidly deployed array of 14 stations, including data for one of the largest aftershocks, an M 6.1 event that occurred on October 27.

Hypocenter distribution of aftershocks

Continuous data recorded from 18:00 (JST) on October 24 to 20:00 October 27 were processed according to the preliminary JMA catalogue (Sakai et al., 2005). We have

about 600 aftershocks with magnitudes ranging from 2.0 to 6.1 in the present study. Due to the strong lateral heterogeneity across the Shibata-Koide Line (SKL) to the east of the Niigata sedimentary basin, we located aftershocks using two one-dimensional velocity models derived previously for this area based on a refraction study (Takeda et al., 2005): a fast-speed model for stations east of the SKL, and a slow-speed model for stations west of the SKL. The earthquake location code was a modified version of *Hypomh* (Hirata and Matsu'ura, 1987). Station corrections were determined for the *P*- and *S*-wave arrival times recorded by the temporary and permanent stations in the vicinity of the source area. Station corrections were also estimated for the permanent stations for location of the mainshock and the three M 6+ aftershocks that occurred before deployment of the temporary array.

The aftershocks were distributed 35 km along the NNE-SSW strike of the geological structure within a 20 km-wide zone, all located between the SKL and the Yukyuzan fault bounding the Uonuma Hill to the west (Fig. 3). The vertical cross-section of the hypocenter distribution is shown in Fig. 4. The distribution reveals two steep west-dipping fault planes about 5 km apart, perpendicular to one east-dipping plane. The mainshock occurred at the deepest extent of the western west-dipping plane, while the largest aftershock (M 6.5) occurred on the eastern west-dipping plane. The M 6.1 aftershock that occurred on the 27th was located at the deepest extent of the east-dipping plane. The shallow extension of the largest aftershock source fault coincides with the SKL (Muikamachi fault), although the aftershocks were limited at depths greater than 8 km. Thus, the mainshock and largest aftershocks occurred on different faults, potentially related to the surface geology. This is one of reason for the large number of aftershocks for this event compared to typical M 6-class earthquakes.

Discussion

The SKL lies to the east of the source area of the mainshock and forms the eastern boundary of the Niigata basin. The SKL was created in the Miocene and was reactivated as the Muikamachi active fault by crustal shortening from 3.5 Ma. The Obiro fault on the eastern boundary of the Uonuma Hill intrudes from the northern extension of the Muikamachi fault. The hill hosts many fault-and-fold structures formed during back-arc rifting associated with the opening of the Japan Sea and subsequently reactivated by inversion tectonics (Sato, 1994).

Kato et al. (2005) determined the seismic velocity structure by the double-difference tomography (Zhang and Thurber, 2003) using the present data (Fig. 5). If we have densely distributed earthquakes in the studied area, the method enables us to have better spatial resolution of the velocity structure than a conventional tomography method within the area of many aftershocks. The tomogram clearly reveals that the lateral variation in seismic velocity extends to depths of 10 km or more, and that the source fault of the mainshock is located on the boundary between the high- and low-velocity zones. The east-dipping fault plane is located at a region of relatively low velocity in the high-velocity body. The relationships suggest that the lateral variation of geology observed at the surface may extend to depth, forming weak zones that may fracture under E-W compression. This interpretation of strong heterogeneity of the source area from the surface to a depth of 15 km may explain the large number of aftershocks that occurred following the present earthquake. This heterogeneity, which extends to the base of the seismogenic layer and which reflects the geological origins of the area (deformed back-arc opening crust and reactivation by inversion tectonics), provides

many weak zones as candidates for moderate to large earthquakes. Furthermore, the source area is located on the Niigata-Kobe tectonic line, which is subjected to significant E-W compression (Sagiya et al., 2000; Iio et al., 2004). This combination of extensive deformation and compression from geological age to the present is therefore considered to be responsible for the strong heterogeneity and high potential seismic activity of the Mid-Niigata area.

Conclusion

From observations of the aftershocks of the 2004 Mid-Niigata Prefecture Earthquake using a temporary seismic array, three major source faults responsible for the mainshock and two major aftershocks were identified. Two of the faults, the source faults of the mainshock and largest aftershock, are parallel, steep west-dipping faults located approximately 5 km apart, while the other fault dips eastward and is oriented perpendicular to the west-dipping faults. Tomographic analysis revealed that the lateral variation of seismic velocity observed at surface extends to a depth of 15 km, encompassing the source area of the mainshock. The strong heterogeneity of the crust is considered to be related to the geological and tectonic evolution of the area, and to provide a setting with numerous potential sites for moderate to large earthquakes. The prominent aftershock activity following the 2004 Mid-Niigata Prefecture Earthquake can therefore be attributed to the highly heterogeneous crustal structure of this area, coupled with E-W compression along the Niigata-Kobe tectonic line.

Acknowledgements

This work is supported by a Grant-in-Aid for Special Purposes (16800054),and

the Special Coordination Funds for the Promotion of Science and Technology (MEXT, Japan) titled as the Urgent Research for the 2004 Mid-Niigata Prefecture Earthquake, and a grant offered under the Earthquake Prediction Research program of the MEXT, Japan. Gratitude is extended to T. Iwasaki, T. Kanazawa, H. Hagiwara, T. Iidaka, T. Igarashi and staff of the Earthquake Research Institute, University of Tokyo, for valuable discussion.

References

Coordinate Committee for Earthquake Prediction Research (2004) Observations of the 2004 Mid-Niigata Prefecture Earthquake. http://www.eri.u-tokyo.ac.jp/YOTIKYO/niigata/index-open.htm

Earthquake Research Institute, University of Tokyo (2004) A report for the 160th Coordinate Committee for Earthquake Prediction (Nov. 4, 2004). http://www.eri.u-tokyo.ac.jp/hirata/chuetsu/0401104yotiren1.htm

Geological Information Center (1991) Geological Map of Nagaoka, 1:50,000

Headquarters for Earthquake Research Promotion (1999) The Promotion of Earthquake Research, Basic comprehensive policy for the promotion of earthquake observation, measurement, surveys and research (in Japanese with English translation)

Hirata N, Matsu'ura M (1987) Maximum likelihood estimation of hypocenter with origin time eliminated using non-linear inverse technique. Phys. Earth Planet. Inter., 47: 50-61

Hirata N, Ohmi S, Sakai S, Katsumata S, Matsumoto S, Takanami T, Yamamoto A, Nishimura T, Iidaka T, Urabe T, Sekine M, Ooida T, Yamazaki F, Katao H, Umeda

Y, Nakamura M, Seto N, Matsushima T, Shimizu H, Japanese University Group of the Urgent Joint Observation for the 1995 Hyogo-ken Nanbu Earthquake (1996) Urgent joint observation of aftershocks of the 1995 Hyogo-ken Nanbu Earthquake, *J. Phys. Earth*, 44: 317-328

Hirata N, Sato H, Research Group for the Urgent Aftershock Observation of the Earthquake Research Institute, University of Tokyo (2005) The 2004 Mid-Niigata Prefecture Earthquake – Source faults estimated by the subsurface structure and aftershocks, Kagaku, ***75***:149-151.

Ikeda Y, Imaizumi T, Togo M, Hirakawa H, Miyauchi Y, Sato H (2002) Atlas of Quaternary thrust faults, Tokyo Univ. Press, 254p

Iio Y, Sagiya T, Kobayashi Y (2004) Origin of the concentrated deformation zone in the Japanese Islands and stress accumulation process of intraplate earthquakes, *Earth Planets Space*, **56**: 831-842

Kato A, Kurashimo E, Hirata N, Iwasaki T, Kanazawa T (2005) Imaging the source region of the 2004 Mid-Niigata prefecture earthquake and the evolution of a seismogenic thrust-related fold, *Geophys. Res. Lett.* (in press)

Matsuda, T. (1995): Active faults, Iwanami-shinsho 423, Iwanami Shoten, 242p.

Maruyama T, Fusejima Y, Yoshioka T, Awata Y and Matsu'ura T (2005), Characteristics of surface rupture associated with the 2004 Mid Niigata Prefecture earthquake, central Japan and their seismotectonic implications, submitted to *Earth, Planets, and Space*.

Natural Gas Mining Society and the Society of Exploration for Oil in the Continental shelf (1992) Oil and natural gas resources in Japan (revised), 520p

Obara K, Hori S, Kasahara K, Okada Y, Aoi S (2000) Hi-net: High sensitivity

seismograph network in Japan, Eos Trans. AGU, 81(48), Fall Meet. Suppl., Abstract S71A-04.

Sakai S., Hirata N, Kato A, Kurashimo E, Iwasaki T, and Kanazawa T (2005), Multi-fault system of the 2004 Mid-Niigata Prefecture Earthquake and its aftershocks, submitted to *Earth, Planets, and Space*.

Sato H, (1994) The relationship between late Cenozoic tectonic events and stress field and basin development in northeastern Japan, J. Geophys. Res., 99: 22261-22274

Sagiya T, Miyazaki S, Tada T (2000) Continuous GPS array and present-day crustal deformation of Japan, Pure Appl. Geophys., 157: 2303-2322

Takeda T, Sato H, Iwasaki T, Matsuta N, Sakai S, Iidaka T., Kato A (2005) Crustal structure in the northern Fossa Magna region, central Japan, from refraction/wide-angle reflection data, Earth Planetary Science (in press).

Tsutsumi H, Togo M, Watanabe M, Kin T, Sato N (2001) Active fault map in urban area: Nagaoka, Technical report of the Geographical Survey Institute, D.1, No. 388

Zhang Z, Thurber CH (2003) Double-difference tomography: the method and its application to the Hayward fault, California, Bull. Seism. Soc. Am., 93: 1875-1889

Fig. 1. Epicenter of the 2004 Mid-Niigata Prefecture Earthquake, with the focal mechanism shown inset as a stereo projection on the lower focal hemisphere, in which shaded areas indicate tension and white areas indicate compression. The mechanism shows a thrust faulting. Solid lines denote the 11 noteworthy active faults in Japan (Matsuda, 1995), among which the western Nagaoka-plane fault system (indicated by an arrow) is the nearest active fault.

Fig. 2. Active faults near the source area of the 2004 Mid-Niigata Prefecture Earthquake. Red solid lines denote active faults (Geological Information Center, 1991; Tsusumi et al., 2001; Ikeda et al., 2002). The Muikamachi and Obirou faults are located on the eastern boundary of Uonuma Hill.

Fig. 3. Epicenteral distribution determined from the present aftershock observation [18:00 JST Oct. 24 to 20:00 JST Oct. 27, 2004; data from Sakai et al.(2005)]. Aftershocks are denoted by color according to depth. There are 625 aftershocks plotted, among which the mainshock and large aftershocks are denoted by circles with numerals: ①M 6.8 mainshock (17:56 Oct. 23), ② M 6.3 aftershock (18: 03 Oct. 23), ③ M 6.0 aftershock (18:11 Oct. 23), ④ M 6.5 aftershock (18:34 Oct. 23), ⑤ M 6.1 aftershock (10:40 Oct. 27). Focal mechanisms are shown as projections on the lower focal hemisphere, where shaded areas indicate tension and white areas indicate compression. Active faults are denoted by solid pink lines.

Fig. 4 Estimated geological cross-section showing the depth distribution of aftershocks determined from the present aftershock observation (see Fig. 3; after Hirata et al., 2005). ①M 6.8 mainshock (17:56 Oct. 23), ② M 6.3 aftershock (18: 03 Oct. 23), ③ M 6.0 aftershock (18:11 Oct. 23), ④ M 6.5 aftershock (18:34 Oct. 23), ⑤ M 6.1 aftershock (10:40 Oct. 27). Triangles denote location of wells of the Natural Gas Mining Society and the Society for Exploration for Oil on the Continental shelf (1992) and the Geological Information Center (1991). Colored solid lines indicate the three major source faults.

Fig. 5 P-wave velocity model (contour interval: 0.25 km/s) on the cross-section along the line A–B in Fig. 3 (after Kato et al., 2005) derived from data recorded by the 14 temporary stations of the present aftershock observation and 43 permanent stations.

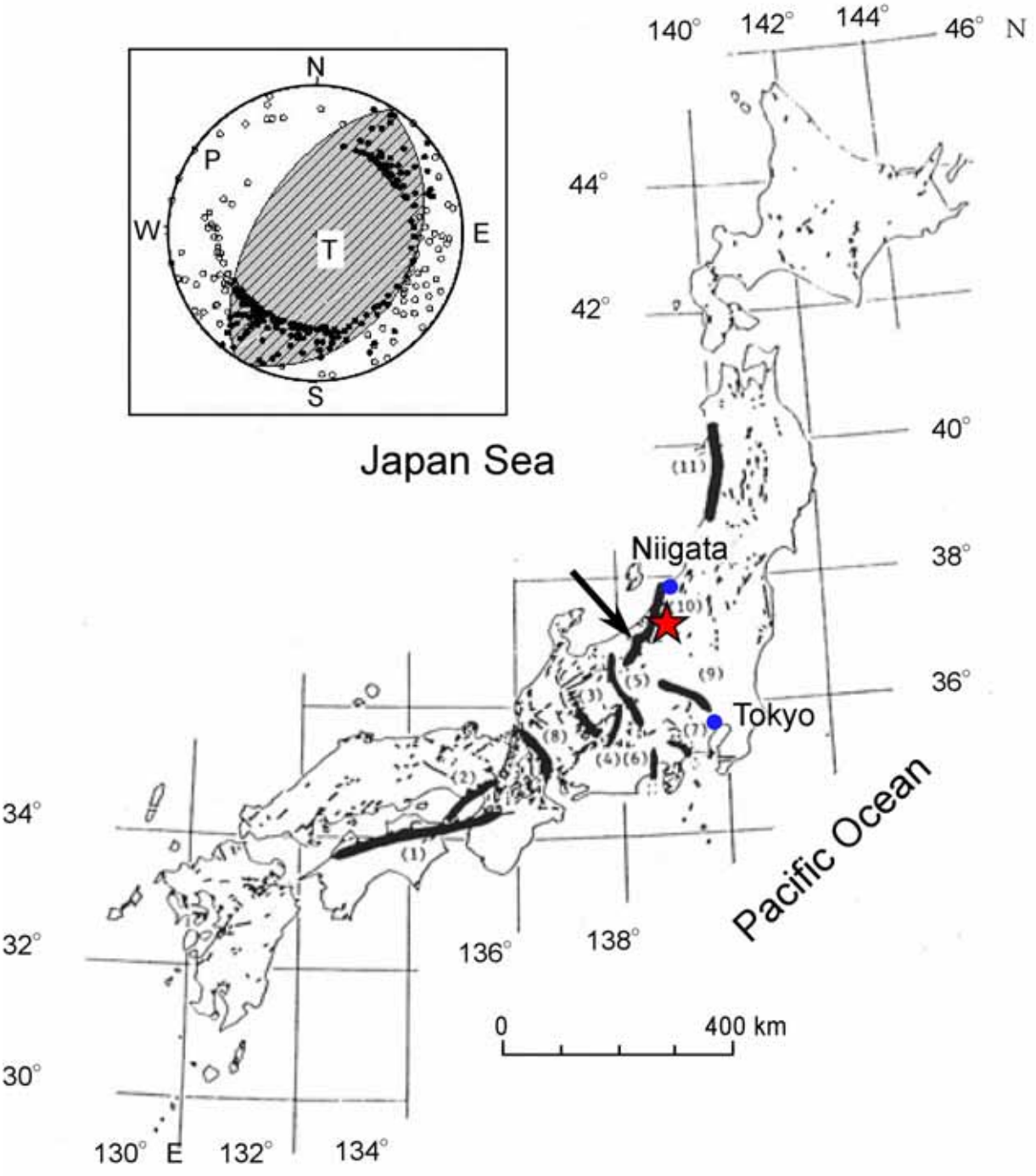
N
P
W
E
T
S
140°
142°
144°
46° N
44°
42°
40°
38°
36°
34°
32°
30°
130° E
132°
134°
136°
138°
Japan Sea
Pacific Ocean
Niigata
Tokyo
(1)
(2)
(3)
(4)(6)
(5)
(7)
(8)
(9)
(10)
(11)
0
400 km

Fig. 1

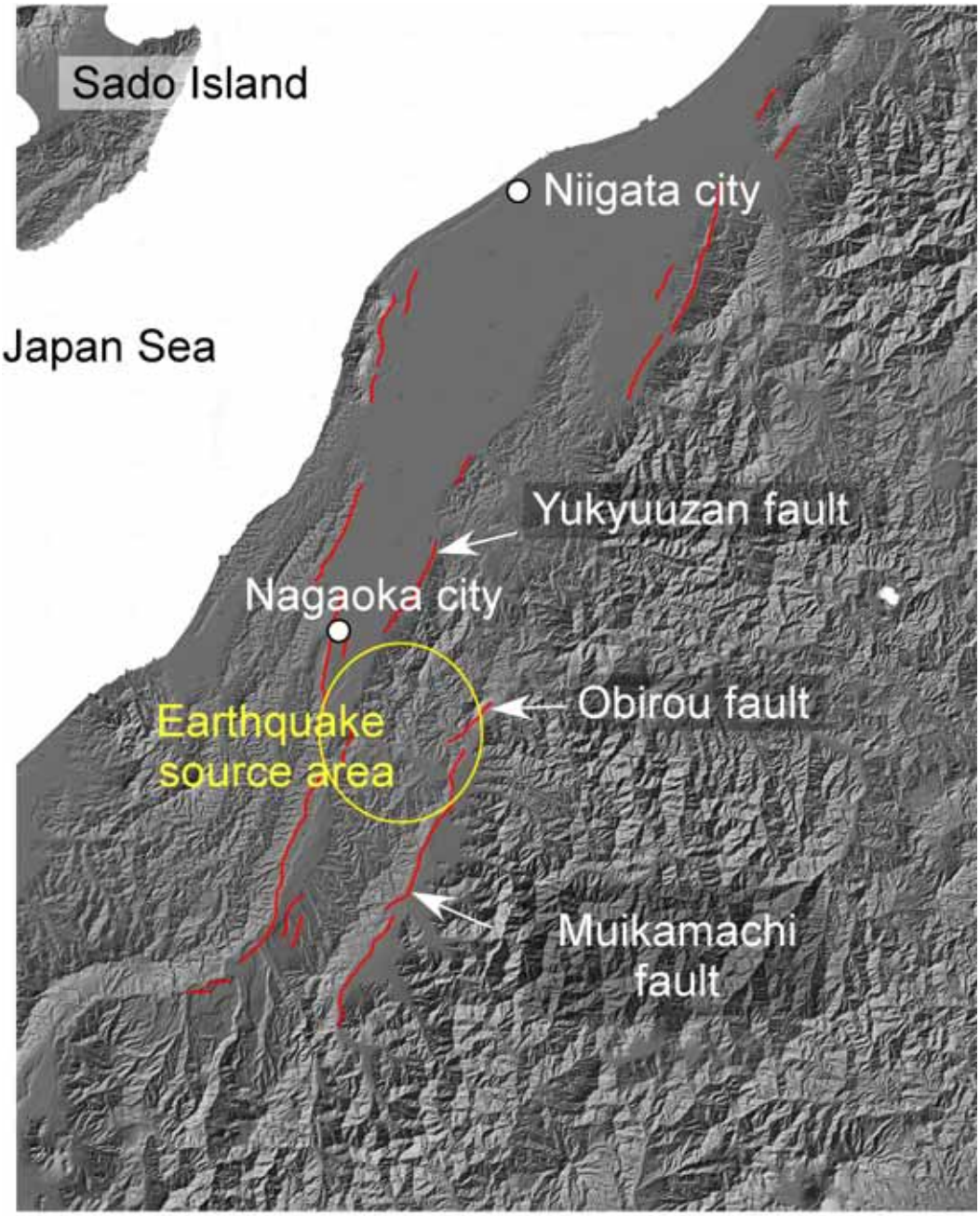
Sado Island
Niigata city
Japan Sea
Yukyuuzan fault
Nagaoka city
Earthquake
source area
Obirou fault
Muikamachi
fault

Fig.2

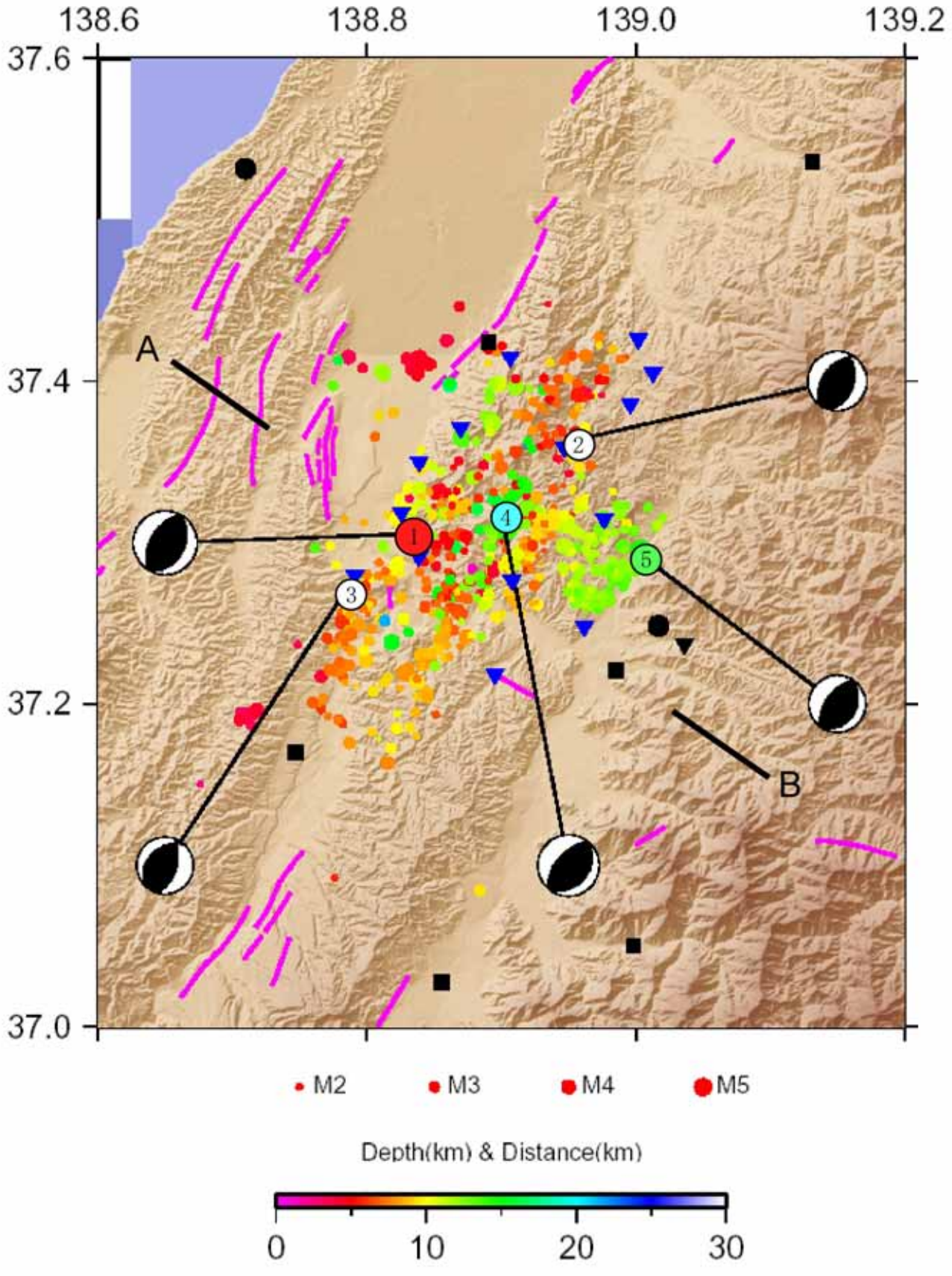
138.6
138.8
139.0
139.2
37.6
37.4
37.2
37.0
A
B
1
2
3
4
5
M2
M3
M4
M5
Depth(km) & Distance(km)
0
10
20
30

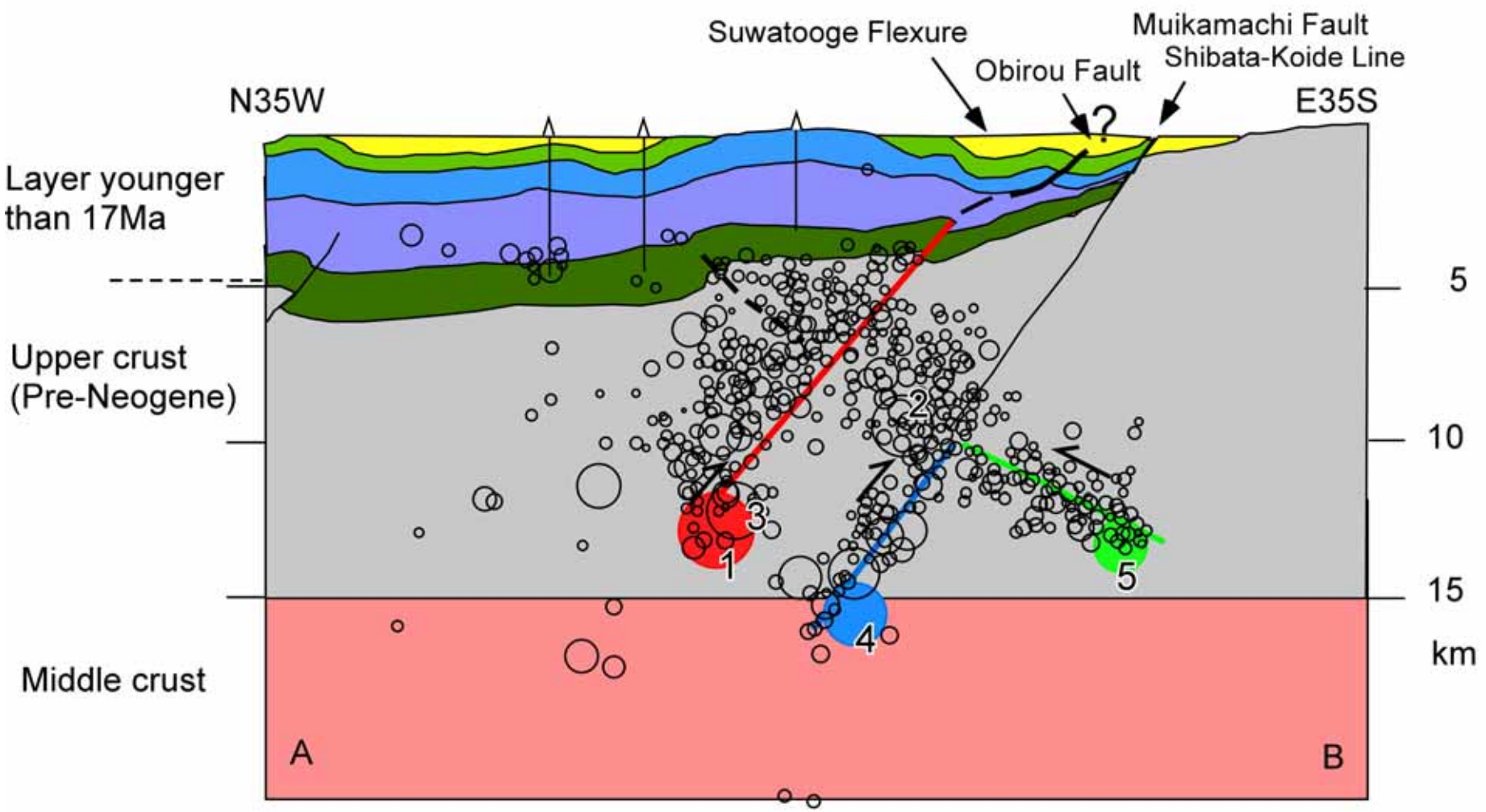
Suwatooge Flexure
Muikamachi Fault
Shibata-Koide Line
Obirou Fault
?
N35W
E35S
Layer younger than 17Ma
Upper crust (Pre-Neogene)
Middle crust
A
B
1
2
3
4
5
5
10
15
km

Fig.4

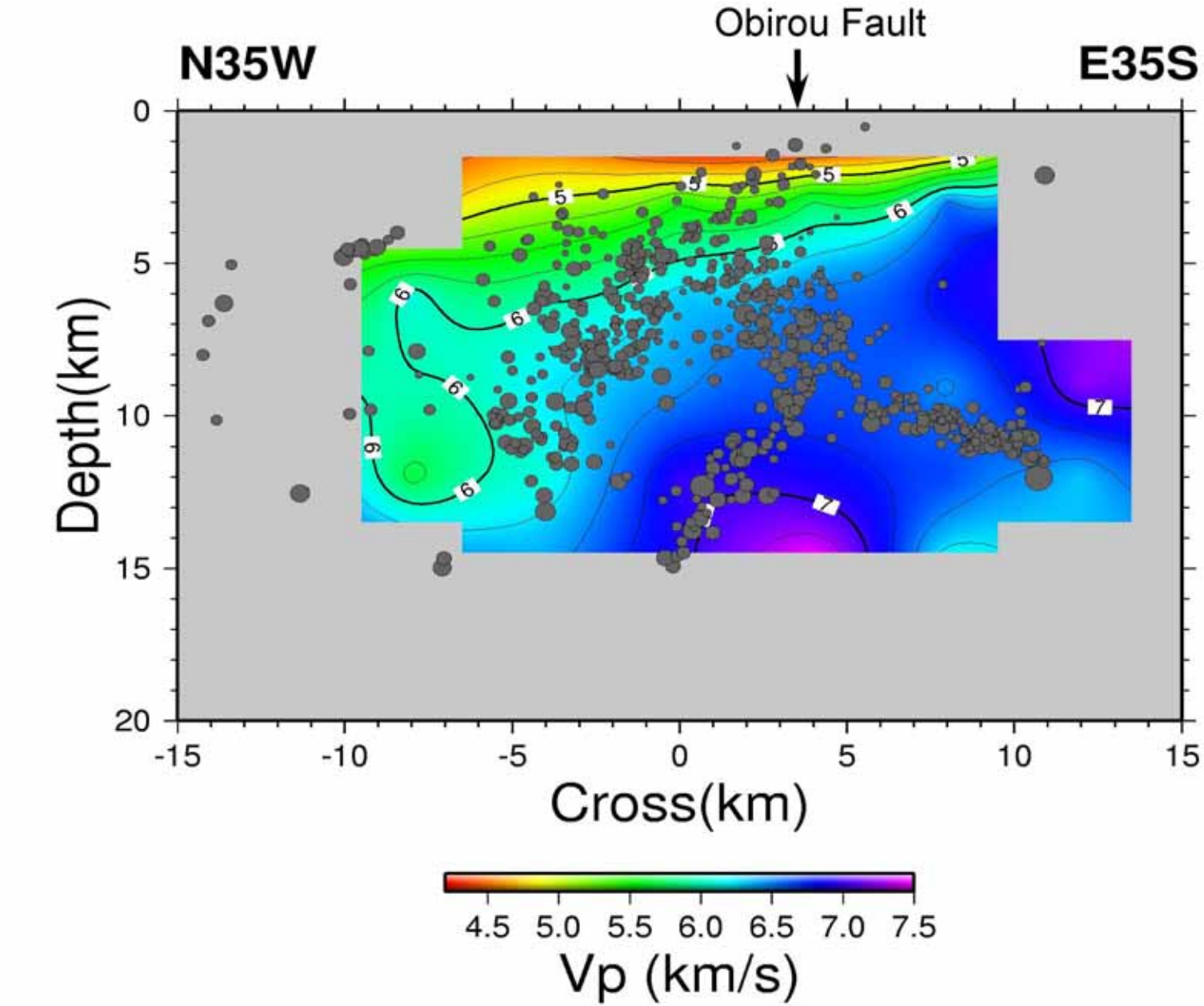
Obirou Fault
N35W
E35S
Depth(km)
0
5
10
15
20
-15
-10
-5
0
5
10
15
Cross(km)
4.5
5.0
5.5
6.0
6.5
7.0
7.5
Vp (km/s)